Received: 30 June 2023 | Revised: 4 September 2023 | Accepted: 5 September 2023

DOI: 10.1002/pamm.202300156

PAMM Proceedings in Applied Mathematics and Mechanics

RESEARCH ARTICLE

Extended integral boundary layer method for reactive species mass transfer in rotating films

Simon Kebinger | **Helfried Steiner** | **Günter Brenn**

Institute of Fluid Mechanics and Heat Transfer, Graz University of Technology, Graz, Austria

Correspondence
Helfried Steiner, Graz University of Technology, Institute of Fluid Mechanics and Heat Transfer, Inffeldgasse 25F, 8010 Graz, Austria.
Email: helfried.steiner@tugraz.at

Funding information
Austrian Research Promotion Agency, Centre of Electrochemical and Surface Technology (CEST), Grant/Award Number: 1.180.000

Abstract
The present work extends the Integral Boundary Layer (IBL) Method to centrifugal force driven thin film flow with mass transfer. The proposed hybrid approach combines the IBL based solution of the flow field with a Finite Difference based solution of the mass transport equation, avoiding any concentration profile assumptions and restrictions on surface chemistry. In comparison against results from highly resolved Computational Fluid Dynamics (CFD) simulations, the proposed concept is proven as a computationally efficient and accurate method well applicable to infinitely fast surface reactions as well as finite rate kinetics.

1 | INTRODUCTION

Centrifugal force driven thin films can be found in a variety of industrial applications. One important example is wet chemical etching and cleaning of silicon wafers in the semiconductor manufacturing industry. The employed spinning disk devices allow for a controlled and uniform treatment of large surface areas and require only little operating liquid and chemicals due to efficient species mass transfer. Figure 1 sketches a typical film flow configuration on a spinning disk.

A liquid jet, carrying the chemical agent, vertically impinges on the centre of the spinning disk and further spreads as a thin liquid film over the disk surface, driven by centrifugal forces. The numerically discretized solution of the full set of the problem governing balance equations (Computational Fluid Dynamics, or CFD, solution) is highly challenging. First, there is a large disparity of the relevant length scales in the radial and vertical directions, which both need to be adequately resolved. Additionally, species transport is often associated with very low diffusivities. The resulting very thin concentration boundary layers further increase the demand on numerical resolution. In view of these difficulties, various computational investigations employed approximate solutions based on the Thin Film Approximation (TFA), mostly solving the reduced formulation with the Integral Boundary Layer (IBL) method. Among these, Rauscher et al. derived an asymptotic solution in the limits of large radii [1]. Kim & Kim investigated smooth film conditions, as well as the onset of waviness [2]. In a further comprehensive stability analysis, Sisoev et al. extensively studied the formation and evolution of capillary waves [3]. Later, the IBL based solution of the TFA formulation was also extended to heat and species mass transfer. Prieling & Steiner investigated the mass transfer in thin wavy films on rotating disks in the limit of large Dahmköhler numbers, as well as heat transfer [4]. Matar et al. considered the absorption of a gas into a wavy liquid film [5]. Basu & Cetegen investigated the heat transfer in spinning films with low inertia and rotation rates, where a hydraulic jump

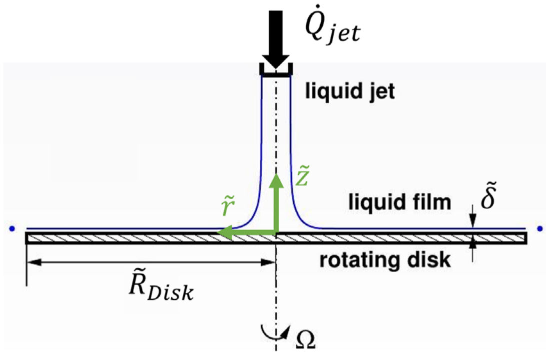

FIGURE 1 Typical configuration for a liquid jet impinging on a spinning disk.

is formed [6]. While Matar et al. only considered iso-value (Dirichlet type) boundary conditions for the scalar transport, Prieling & Steiner, as well as Basu & Cetegen, also prescribed iso-flux (von Neumann type) boundary conditions.

The goal of the present work is to propose an extension of the TFA-IBL model from momentum transport to species mass transport, which readily allows for any wall boundary conditions, covering the full range from infinitely fast to slow finite rate reactions.

2 | FUNDAMENTALS OF THE TFA-IBL APPROACH

As shown in figure 1, we consider the steady axisymmetric flow of a thin liquid film over a disk, which is supplied at the center of rotation by a vertically impinging jet. The volumetric flow rate is $\dot{Q}$, the radius of the disk is $\tilde{R}_{Disk}$. The liquid is Newtonian and incompressible. The angular velocity of the substrate is denoted by Ω. Rescaling the flow variables as

$$r = \tilde{r}/l_0,\ z = \tilde{z}/\delta_0,\ u = \tilde{u}/u_0,\ v = \tilde{v}/v_0,\ w = \tilde{w}/w_0,\ p = \tilde{p}/p_0 \tag{1}$$

with the reference quantities introduced by Rauscher et al. [1]

$$l_0 = \left(\frac{9\dot{Q}^2}{4\pi^2\Omega\nu}\right)^{1/4},\ \delta_0 = \left(\frac{\nu}{\Omega}\right)^{1/2},\ u_0 = v_0 = \Omega l_0,\ w_0 = \Omega\delta_0,\ p_0 = \rho\Omega^2 l_0^2 \tag{2}$$

the considered steady axisymmetric smooth film flow can be described by the following non-dimensional balance equations for mass and momentum in a cylindrical coordinate system, rotating with Ω around the z-axis:

$$\frac{1}{r}\frac{\partial ru}{\partial r} + \frac{\partial w}{\partial z} = 0 \tag{3}$$

$$\frac{1}{r}\frac{\partial ruu}{\partial r} + \frac{\partial uw}{\partial z} - \frac{v^2}{r} = -\frac{\partial p}{\partial r} + 2v + r + \frac{\partial^2 u}{\partial z^2} + O(\epsilon^2) \tag{4}$$

$$\frac{1}{r}\frac{\partial ruv}{\partial r} + \frac{\partial vw}{\partial z} + \frac{uv}{r} = -2u + \frac{\partial^2 v}{\partial z^2} + O(\epsilon^2) \tag{5}$$

$$0 = -\frac{\partial p}{\partial z} - \epsilon Fr^{-1} \tag{6}$$

Consistent with the smooth film assumption, the influence of surface tension is neglected. The Froude number is defined as $Fr = \Omega^2 l_0/g$. As such, the shown formulation (3)–(6) represents the TFA, where the terms of $O(\epsilon^2)$ are neglected, due to the small aspect ratio $\epsilon = \delta_0/l_0 \ll 1$.

The spatial dependence of the quantities in the TFA formulation on the vertical coordinate z is eliminated by applying the *IBL* (IBL) method, which considers only depth-averaged quantities over the non-dimensional film thickness $\delta = \tilde{\delta}/\delta_0$, generally defined as:

$$\bar{\Phi}(r) = \frac{1}{\delta}\int_0^\delta \Phi(r,z)\,dz \tag{7}$$

Depth-averaging Equations (3)–(6) with the boundary conditions

$$\text{no slip}:z = 0: \; u = v = w = 0 \tag{8}$$

$$\text{kinematic}:z = \delta: \; w = u\frac{\partial\delta}{\partial r} \tag{9}$$

$$\text{zero stress at free surface}:z = \delta: \; \frac{\partial u}{\partial z} = \frac{\partial v}{\partial z} = 0 \tag{10}$$

yields the following set of equations for the film thickness and the depth-averaged radial and azimuthal velocities written as

$$\frac{1}{r}\frac{\partial}{\partial r}\begin{pmatrix} r\delta\bar{u} \\ k_a r\delta\bar{u}^2 \\ k_b r\delta\bar{u}\bar{v}\end{pmatrix} = \begin{pmatrix} 0 \\ k_c\delta\bar{v}^2/r + 2\delta\bar{v} + b_1(r - \frac{\epsilon}{Fr}\frac{\partial\delta}{\partial r})\delta - b_2\bar{u}/\delta \\ -k_b\delta\bar{u}\bar{v}/r - 2\delta\bar{u} - 5\bar{v}/(2\delta)\end{pmatrix} \tag{11}$$

only dependent on r. The parameters k_a, k_b, k_c, b_1 an b_2 are determined by the profile functions

$$u(\zeta) = \frac{5}{16}\bar{u}(8\eta - 4\eta^3 + \eta^4) + \frac{\kappa\delta^2}{10}\left(\frac{7}{3}\eta - 5\eta^2 + \frac{23}{6}\eta^3 - \frac{23}{24}\eta^4\right) \tag{12}$$

$$v(\zeta) = \frac{5}{16}\bar{v}(8\eta - 4\eta^3 + \eta^4) \tag{13}$$

which need to be assumed for describing the z-dependency of the integrands in the depth-averaging (Equation 7). The rescaled wall coordinate η is defined as

$$\eta = \begin{cases} z/\delta_r & \delta_r < \delta \\ z/\delta & \delta_r = \delta \end{cases} \tag{14}$$

where δ_r represents the non-dimensional radial velocity boundary layer. The chosen fourth-order polynomials follow a suggestion of Kim & Kim [2]. The profile parameter κ is given by $\kappa = r - \partial p/\partial r|_{z=0}$. Close to impingement, where $\delta_r < \delta$, a radially variable free stream velocity $u_\infty(r)$ was used, which was taken from a potential flow solution proposed by Miyasaka [7].

3 | EXTENSION OF TFA-IBL METHOD TO MASS TRANSFER

Using the scalings introduced by Equation (2), the dimensionless TFA approximation of the steady transport equation of a rescaled species mass concentration $c = \tilde{c}/c_{ref}$ in axisymmetric flow reads in cylindrical coordinates

$$u\frac{\partial c}{\partial r} + w\frac{\partial c}{\partial z} = \frac{1}{Sc}\left[\frac{\epsilon^2}{r}\frac{\partial}{\partial r}\left(r\frac{\partial c}{\partial r}\right) + \frac{\partial^2 c}{\partial z^2}\right] \tag{15}$$

Sc is the Schmidt number $Sc = \nu/D$ with the diffusion coefficient D.

Making the model amenable to arbitrary surface chemistry, the wall boundary condition for the species mass flux, which follows from the reactive wall flux $\tilde{J}_{react} = D\,\partial\tilde{c}/\partial\tilde{z}$ at $\tilde{z} = 0$ as stated in literature [8], is generally prescribed as

$$\frac{\partial c}{\partial z}|_{z=0} = Da\; c^n|_{z=0}. \tag{16}$$

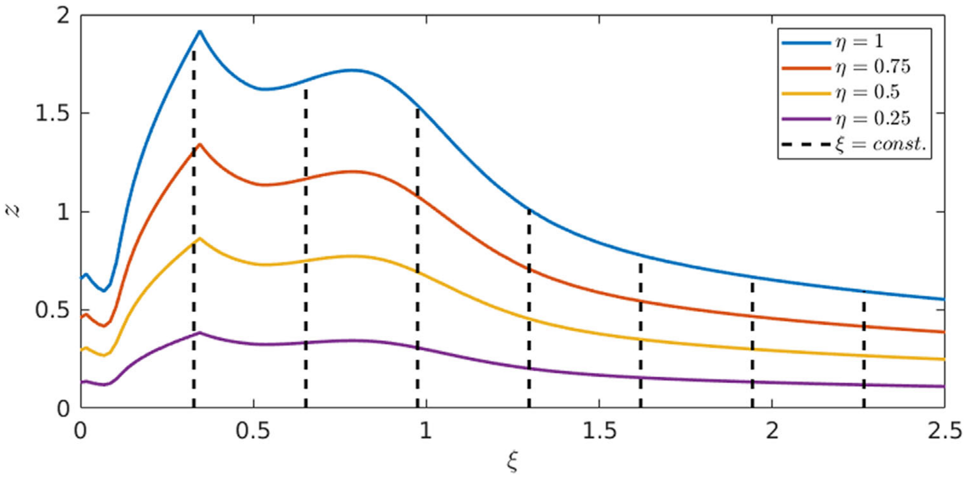

FIGURE 2 Surface fitted coordinate system within the liquid film.

The non-dimensional factor on the right hand side is the Damköhler number. It represents the ratio of the diffusive to the reactive time scales and is defined as

$$Da = \frac{\tau_{diff}}{\tau_{react}} = \frac{\tilde{k}\delta_0 c_{ref}^{n-1}}{D}. \tag{17}$$

As such, the applied ansatz (16) covers the full range from finite-rate reaction with constant or non-constant rate, for finite Da and rate exponent $n = 0$ or $n \neq 0$, respectively, to infinitely fast chemistry, for $Da \to \infty$ and $c|_{z=0} = c_w = 0$.

Using straight-forwardly the IBL method for the mass transfer, the profile function for the concentration substituted into Equation (16) would tightly connect the non-dimensional thickness of the concentration boundary layer δ_c to the rate of reaction at the surface with a determining dependence on the wall gradient of the assumed profile. In the present work we aim to circumvent this restriction, avoiding the use of profile functions. The two-dimensional species mass transport equation (15) is rather solved numerically, discretized with a Finite Difference scheme, using a surface fitted coordinate system with the non-dimensional coordinates $\xi = r$ and η (Equation 14).

The computational domain, with some selected coordinate lines, $\xi = const.$ and $\eta = const.$, is sketched in Figure 2. The line $\eta = 1$ represents the upper boundary, being the radial velocity boundary layer thickness δ_r near the center, and the film thickness δ radially further outside. The thicknesses δ_r and δ, as well as the velocities u and w, were taken from the TFA-IBL solutions of the continuity and momentum equations.

The boundary conditions for the species mass transport in the transformed coordinate system read

$$\text{wall}: \eta = 0: \begin{cases} c_w = 0 & Da \to \infty \\ \dfrac{\partial c}{\partial \eta} = \begin{cases} \delta_r\, Da\, c_w^n & \text{for } \delta_r < \delta \\ \delta\, Da\, c_w^n & \text{for } \delta_r = \delta \end{cases} & \text{finite } Da \end{cases} \tag{18}$$

$$\text{upper boundary}: \eta = 1: \ c = 1 \tag{19}$$

$$\text{radially inner}(\xi_{in} = 10^{-4}): c = \begin{cases} c_w + (1 - c_w)\left[\dfrac{3}{2}\dfrac{\eta}{\eta_c} - \dfrac{1}{2}\left(\dfrac{\eta}{\eta_c}\right)^3\right], \text{for } 0 \le \eta \le \eta_c = 1/\sqrt{Sc} \\ 1, \text{for } \eta > \eta_c \end{cases} \tag{20}$$

$$\text{radially outer}(\xi_{out} = R_{Disk}): \frac{\partial c}{\partial \xi} = 0 \tag{21}$$

A second order accurate central Finite Difference scheme is applied to discretize all spatial derivatives occurring in Equation (15). The obtained system of equations for the concentration c is linearized in the case of non-linear surface reaction

TABLE 1 Flow and reaction conditions.

$\dot{Q}_{jet}$	1.8		$\mathrm{L\,min^{-1}}$
Ω	300		$\mathrm{min^{-1}}$
$\tilde{R}_{Disk}$	0.15		m
μ	$7.432 \cdot 10^{-4}$		$\mathrm{kg\,m^{-1}\,s^{-1}}$
ϱ	1033		$\mathrm{kg\,m^{-3}}$
D	$4 \cdot 10^{-9}$		$\mathrm{m^2\,s^{-1}}$
Sc	180		–
$c_{ref} = c_{jet}$	2.58		$\mathrm{kmol\,m^{-3}}$
Chemistry:	**infinite rate**	**finite rate**	
$\tilde{k}$	∞	$3 \cdot 10^{-5}$	$\mathrm{m^4\,kmol^{-1}\,s^{-1}}$
n	–, ($c_w = 0$)	2	–
$Da = \frac{\tilde{k}\delta_0 c_{ref}^{n-1}}{D}$	∞	2.93	–

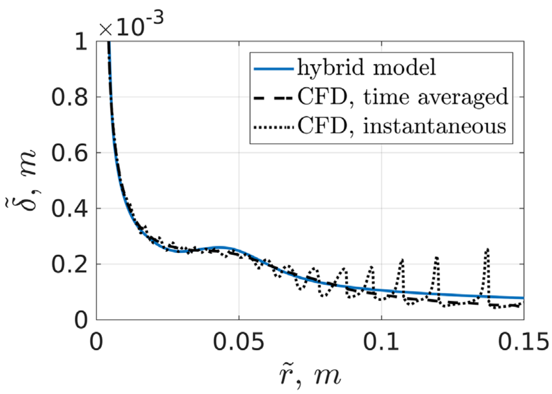

FIGURE 3 Radial variation of film height $\tilde{\delta}$.

rate for $n \neq 1$ in the b.c. (18). The discretized formulation of the present hybrid model was programmed and solved using Matlab.

4 | DISCUSSION OF RESULTS

The proposed hybrid approach was tested for two representative cases, assuming infinitely fast and finite rate surface chemistries. The flow and reaction conditions are listed in Table 1, where the underlying flow conditions are kept the same for both cases. The case with finite rate chemistry is representative for the etching of silicon dioxide with hydrofluoric acid, assuming the reaction mechanism suggested by literature [8, 9]. The data used for validation of the predictions were obtained by highly resolved CFD simulations with the software ANSYS/Fluent, where the full set of the governing equations is numerically solved applying a volume of fluid (vof) two-phase flow model with compressive interface tracking. Given sufficient spatial resolution, the CFD approach provides a most detailed high fidelity description of the flow and concentration fields. As such, it delivers a sound basis for validation, but entailing substantially higher computational costs than the hybrid model.

4.1 | Momentum transport

The film thickness and the wall shear stress are tightly connected with momentum transfer, which makes them both good indicators for assessing the accuracy of the predicted flow field. As seen from the predicted radial variations of these quantities in Figures 3 and 4, the TFA-IBL model apparently describes the momentum transfer very well. We generally see close

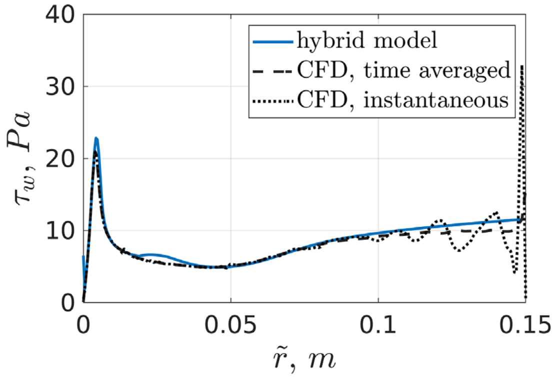

FIGURE 4 Radial variation of wall shear stress τ_w.

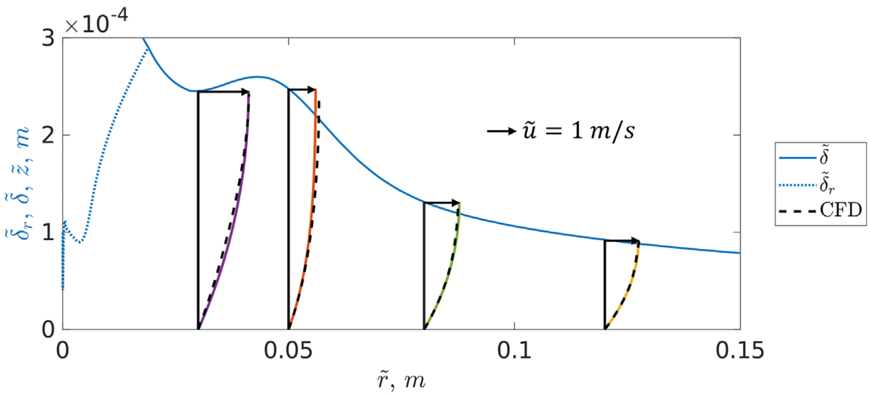

FIGURE 5 Profiles of radial velocity $\tilde{u}$ at selected radial positions.

agreement with the validation data from CFD. The hump due to the decelerating effect of viscous friction is predicted more pronounced by the TFA-IBL model. Moreover, assuming steady smooth film flow, the TFA-IBL model inherently does not predict the formation of capillary waves in the radially outer regions as featured by the instantaneous CFD data. For the most part of the domain the time averaged representations are still reproduced very well. The consistently somewhat lower average films thickness of the CFD data in the radially outer region can be attributed to the increased radial throughput of liquid mass, which effectively reduces the mean height of wavy films as compared to their smooth counterparts.

Figure 5 compares radial velocity profiles at selected radial positions. The quartic profile function, Equation (12), presently assumed by the TFA-IBL model, evidently approximates the validation data from CFD very well.

4.2 | Species mass transport

As explained above, the hybrid approach circumvents any profile assumption for the z-dependence of the species concentration c by solving the species mass transport equation differently from the TFA-IBL concept. Solving for the concentration field with a Finite Difference method instead provides more flexibility in handling different types of surface chemistry. Figures 6 and 7 display profiles of the species concentration at selected radial positions. The predictions of the hybrid model are evidently in very good agreement with the high-fidelity CFD results for both Damköhler number cases.

The close agreement observed for all the profiles is also reflected by the predicted wall concentration in the finite rate case, as shown in Figure 8. Some deviations are seen only in close proximity to the center. This is not surprising, as the simplifying assumptions of TFA apply only in the radially outer thin film region, while they break down in the central region beneath the vertically impinging jet. The assumed surface chemistry essentially determines the into-wall flux of the

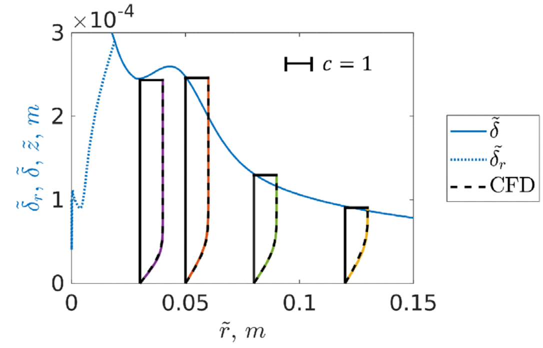

FIGURE 6 Profiles of species mass concentration at selected radial positions for $Da \to \infty$.

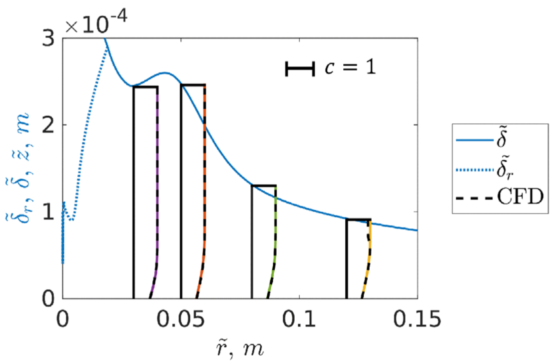

FIGURE 7 Profiles of species mass concentration at selected radial positions for the finite $Da = 2.93$.

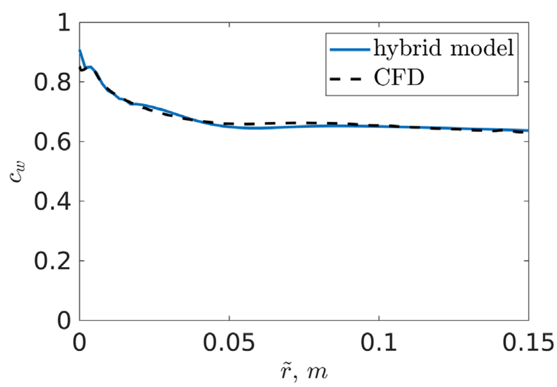

FIGURE 8 Species mass concentration on the disk surface; $c_w = c(r, z = 0)$ for finite rate chemistry, $Da = 2.93$.

reactive species. The corresponding transfer rate is commonly parameterized in terms of the Sherwood number, defined as

$$Sh = \frac{\frac{\partial c}{\partial z}|_{z=0}}{1 - c_w}. \tag{22}$$

The predicted radial variation of this important non-dimensional transfer parameter is shown in Figure 9. Excellent agreement with the CFD results is observed again for most part of the domain in both Damköhler number cases. The deviations appearing very next to the centre point once more at the limited validity of the TFA assumptions in this region, combined with the principal difficulty of imposing appropriate mass inflow conditions at the inner radial boundary very close to singularity at $r = 0$. It is also noteworthy that, despite the strong differences in the rates of the chosen surface reactions (see Table 1), the resulting variations of Sh only differ marginally for the two cases. The significantly reduced

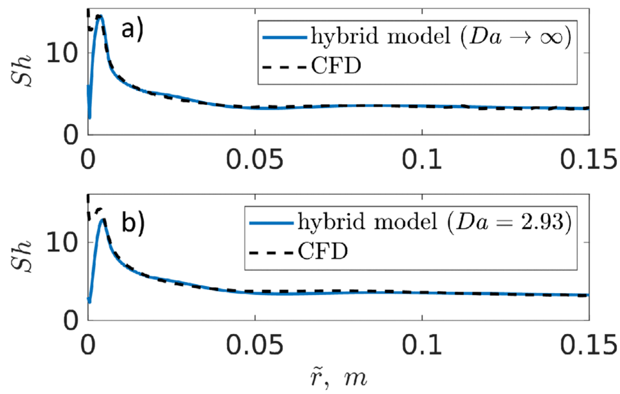

FIGURE 9 Radial variation of the Sherwood number Sh: (A) infinite rate, (B) finite rate chemistry.

into-wall flux due to the decreased consumption of reactive species by the slower finite rate chemistry is apparently largely compensated by an equivalently reduced bulk-to-wall difference $1 - c_w$, as c_w is increased.

5 | CONCLUSIONS

In accordance with past studies, we found the TFA-IBL model to be a reliable approach for predicting accurately the velocity field in centrifugal force driven rotating films. The presently proposed hybrid extension to species mass transfer, combining the TFA-IBL based solution for momentum with the Finite Difference based solution for mass transport, was shown as a well suited flexible concept, which is amenable to arbitrary surface chemistry and the associated boundary conditions. The validation against high-fidelity data from well resolved CFD simulations proved the hybrid model as an accurate, robust, and computationally efficient alternative to the inherently more expensive CFD approach. A further extension of the model considering also reactions within the liquid film is ongoing work.

ACKNOWLEDGMENTS

The authors would like to gratefully acknowledge funding by the Austrian Research Promotion Agency FFG (WetCleanSim program, project number 865864) and the industrial partner LAM Research AG.

ORCID

Simon Kebinger https://orcid.org/0000-0001-6359-7877

REFERENCES

1. Rauscher, J. W., Kelly, R. E., & Cole, J. D. (1973). An asymptotic solution for the laminar flow of a thin film on a rotating disk. *Journal of AppliedMechanics*, *43*, 43.
2. Kim, T. S., & Kim, M. U. (2009). The flow and hydrdynamic stability of a liquid film on a rotating disc. *Fluid Dynamics Research*, *41*, 28.
3. Sisoev, G. M., Matar, O. K., & Lawrence, C. J. (2003). Axisymmetric wave regimes in viscous liquid film over a spinning disk. *Journal of Fluid Mechanics*, *495*, 385.
4. Prieling, D., & Steiner, H. (2013). Analysis of the wall mass transfer on spinning disks using an integral boundary layer metho. *Chemical Engineering Science*, *101*, 109.
5. Matar, O. K., Lawrence, C. J., & Sisoev, G. M. (2005). The flow of thin liquid films over spinning disks: Hydrodynamics and mass transfer. *Physics of Fluids*, *17*, 2051.
6. Basu, S., & Cetegen, B. M. (2007). Effect of hydraulic jump on hydrodynamics and heat transfer in a thin liquid film flowing over a rotating disk analyzed by integral method. *Journal of Heat Transfer*, *129*, 657.
7. Miyasaka, Y. (1974). On the flow of a viscous free boundary jet on a rotating disk: 1st Report Theoretical Analysis. *Bull. JSME 17*, 1461.
8. Monk, D. J., Soane, D. S., & Howe, R. T. (1994). Hydrofluoric acid etching of silicon dioxide sacrificial layers: I. Experimental Observations. *Journal of the Electrochemical Society*, *141*, 270.
9. Bühler, J., Steiner, F.-P., & Baltes, H. (1997). Silicon dioxide sacrificial layer etching in surface micromachining. *Journal of Micromechanics and Microengineering*, *7*, R1.

How to cite this article: Kebinger, S., Steiner, H., & Brenn, G. (2023). Extended integral boundary layer method for reactive species mass transfer in rotating films. *Proceedings in Applied Mathematics and Mechanics*, e202300156. https://doi.org/10.1002/pamm.202300156